

Atomic force microscopy and modeling of natural elastic fibrillin polymers

Eric Hanssen, Suzanne Franc, Robert Garrone

Institut de Biologie et de Chimie des Protéines, CNRS-UPR 412, 7, passage du Vercors,
69367 Lyon cedex 07, France

A central issue in the understanding of Marfan syndrome deals with the functional architecture of fibrillin-containing microfibrils. Fibrillin-rich microfibrils are long extracellular matrix fibrillar components exhibiting a 50 nm periodic beaded-structure with a width of around 20–25 nm after rotary shadowing and a 10–12 nm diameter when observed in ultra-thin sections. They are composed of fibrillin monomers more or less associated with many other components which are, for the most part, poorly characterized up to date. They are known to be elastic but few data have been accumulated to understand their properties. Atomic force microscopy (AFM) allowed us to morphologically differentiate fibrillin-rich microfibrils from other fibrillar components and to investigate the thin structure of these beaded filaments in their native state. They showed, in AFM, a periodic beaded structure ranging from 50 to 60 nm and a width of about 40 nm. The different sizes of fibrillin-containing microfibrils previously observed after rotary shadowing and in ultra-thin sections was resolved with our technique and is revealed to be 10 nm in diameter. Each beaded microfibril appears to be composed of heterogeneous beads connected by 2–3 arms. An orientation of the microfibrils has been shown, and allows us to propose a complementary model of microfibrillar monomer association. (© Elsevier, Paris)

fibrillin / microfibrils / atomic force microscopy / non-contact mode

INTRODUCTION

Elastic properties of animal tissues and some tissue secretions are related to a variety of systems based on biological rubber-like polymers. In invertebrates, different components are involved in the formation of the hinge of bivalves (Kikuchi *et al.*, 1987), the spider's web (Xu and Lewis, 1990) or the mussels byssus (Vitellaro-Zuccarello *et al.*, 1983). In vertebrates, it seems that only two kinds of polymeric proteins are concerned: elastin and fibrillins. Moreover, mixtures of these two kinds of proteins form the major elastic components, elastic fibers and elastic laminae (Rosenblum *et al.*, 1993), encountered in organs. The elasticity of elastin is thought to be due to the high reticulate organization of the polymer itself, which is largely homogeneous. In contrast, the fibrillins are associated with several other glycoproteins to form extensible

beaded microfibrils (Keene *et al.*, 1991), the elasticity of which is much less well understood.

Fibrillin-rich microfibrils (Robert and Robert, 1980) are long, extracellular matrix fibrillar components exhibiting a 55-nm periodic beaded structure (Keene *et al.*, 1991). They have a diameter of about 10–12 nm when observed in ultra-thin sections (Keene *et al.*, 1991) and a width of around 20–25 nm after rotary shadowing (Wright and Mayne, 1988). They are mainly composed of fibrillin (Sakai *et al.*, 1986) associated with other components which are, for the most part, poorly characterized up to date. For example, microfibril-associated glycoprotein-1 (MAGP-1) (Gibson and Cleary, 1987), was detected by immunoelectron microscopy associated with microfibrils at the bead level (Henderson *et al.*, 1996). Other proteins were co-localized with the microfibrils (Kagan *et al.*, 1986; Bressan *et al.*, 1993; Gibson *et al.*, 1995, 1996; Roark *et al.*, 1995; Reinhartd

et al, 1996), and some of them seem to establish a connection with the surrounding matrix. Proteoglycan, as chondroitine sulfate proteoglycan, is also attached to microfibrils (Kielty *et al*, 1996). However, fibrillin remains the main constituent of the microfibrils and has the shape of thin rod-like monomer with 148 nm in length and 2.2 nm in width after rotary shadowing (Sakai *et al*, 1991). When polymerized into microfibrils, the fibrillin monomers are thought to constitute the thin filamentous structures observed between the microfibrillar beads (Wright and Mayne, 1988). Their number has been estimated to be between 6 and 8. However, the observed 55 nm microfibrillar periodicity has never been correlated with the 148 nm-long monomers. The importance of fibrillin has been revealed by the discovery of mutations that led to cardiovascular, ocular and skeletal manifestations of the Marfan syndrome (Dietz *et al*, 1991; Lee *et al*, 1991; Maslen *et al*, 1991; Pyeritz, 1993). These pathologies found expression for example in an aortic dissection and an ectopia lentis and could be due to a loss of extracellular matrix elasticity dependent on a possible disorganization of mutated fibrillin microfibrils.

To increase the available data on fibrillin-containing microfibril organization, we investigated the organization of these microfibrils using atomic force microscopy (AFM) (Binning *et al*, 1986). The AFM image is derived from the vertical deflection of a tip which is rastered across the sample surface in sub-Angstrom increments. The vertical movement of the AFM tip is monitored by a laser beam that is reflected off the back of the tip onto a photodetector grid. While the vertical resolution of the AFM is in the sub-Angstrom range, lateral resolution is lower because of its dependence on parameters such as tip diameter and sample shape (Stemmer and Engel, 1990; Blackford *et al*, 1991). The AFM is distinguished from scanning electron microscopy (SEM) techniques partly because it does not require the sample to be coated, stained, dried or observed under vacuum. Thus, biological materials can be observed in their native state. Of further relevance is that the AFM offers the investigator a quick and precise method of the surface topography quantification (Chernoff and Chernoff, 1992; Baselt *et al*, 1993).

MATERIALS AND METHODS

Microfibril purification

Specimens of bovine nuchal ligament collected from local slaughterhouse, 2 to 4 h after death, were purified according to the method described previously (Kielty *et al*, 1998). Briefly, the ligaments were chopped thinly and then digested by bacterial collagenase type 1A (Sigma-

Aldrich) for 12 h at 4°C. The digested product was centrifuged at 10 000 g for 20 min. The supernatant was applied to a Sepharose CL-2B column (Pharmacia-BioTech). The excluded peak containing large extracellular matrix components was digested by hyaluronidase type 1S (Sigma-Aldrich) for 12 h at 4°C and ultracentrifuged at 30 000 g for 72 h at 15°C. The different fractions were checked by TEM after rotary shadowing. The fibrillin-containing microfibril fractions, free of type VI collagen, were pooled and dialyzed against water prior to observation.

Rotary shadowing observations

Fibrillin-containing fractions were analyzed by TEM after rotary shadowing using the mica sandwich technique described by Mould *et al* (1985). Fibrillin-containing fractions, dialyzed against 0.2 M ammonium acetate pH 6.0, were sandwiched between two sheets of freshly cleaved mica and allowed to absorb onto the mica surfaces for 5 min. The sandwiches were split open and dried *in vacuo*, rotary shadowed with platinum wire on a tungsten filament at an angle of 8° and then coated with carbon (MED 010 Turbo EVM 052, Balzers). The replicas were floated off onto distilled water and picked up on uncoated 300 mesh copper grids. The transmission electron microscopy observations were carried out on a Philips CM120 transmission electron microscope under 80 kV at the 'Centre de Microscopie Electronique Appliquée à la Biologie et à la Géologie' of the University Claude Bernard (Lyon, France).

Atomic force microscopy observations

The study was carried out on an Explorer AFM (TopoMetrix, Darmstadt, Germany) mounted on an elastic isolation table and covered with an acoustic hood. For all our work, microfibrils were imaged in non-contact mode, in air, at room temperature. In this mode, correction of the Z piezoceramic is used to detect sample height. Pictures were obtained with HFR Silicon SFM probes (TopoMetrix).

For imaging, in air and non-contact mode, the microfibril solution was spread on a freshly cleaved mica surface, allowed to adhere during 30 s, washed twice with distilled water and then air-dried prior to observation. The parameters used to identify the fibrillin-containing microfibrils are: morphological, as periodicity and beaded-structure.

Data analysis was carried out using the software SPM Lab 3.06 (TopoMetrix) on 23 images concerning 150 beads. All images presented in this work are representative of statistical data.

RESULTS

Fibrillin-rich microfibrils were easily identified. On AFM images their morphological pattern seems to be the same as that from TEM observation after rotary shadowing. They exhibit a 50–55 nm periodic beaded-structure (fig 1A) which is a known characteristic of these microfibrils after rotary shadowing and observation in transmission electron microscopy (Wright and Mayne, 1988). In AFM (fig 1B, C) a similar periodicity from 50 to 60 nm is

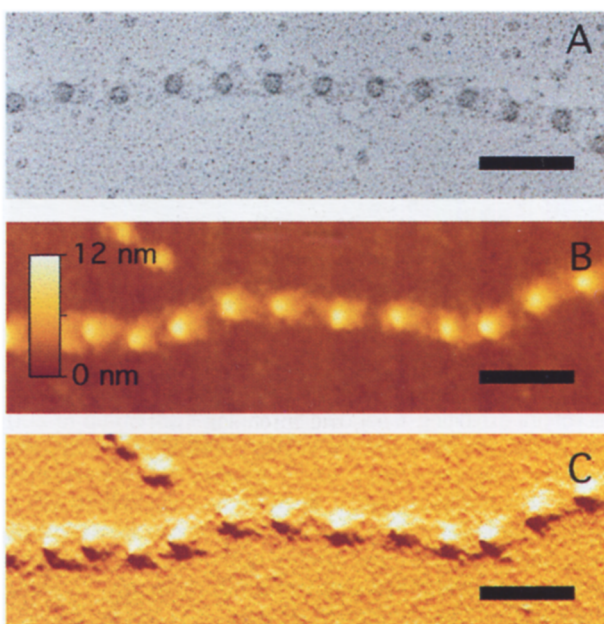


Fig 1. Comparative aspect of fibrillin-containing microfibrils in transmission electron microscopy and atomic force microscopy. **A.** After rotary shadowing and TEM observation, the periodicity is ranging from 55 to 60 nm and the width is about 25 nm. **B.** After AFM observation, fibrillin-rich microfibrils exhibited a 55–60 nm periodicity. Scale shows the sample height ranging from 0 to 12 nm. **C.** Different presentation of **B** using an artificial shadowing generated by SPM Lab 3.06. The two techniques, AFM and TEM, allow to obtain a similar periodic pattern of fibrillin-containing microfibrils. Scale bars, 100 nm.

observed. But the width, which is a function of the tip of the cantilever used, is here around 40 nm, against 25 nm in rotary shadowing.

The AFM image gives the Z data, corresponding to the third dimension in all images obtained. It is thus possible to obtain an apparent height of microfibrils at different sites, and specifically at the level of the beads where it is of 9.5 ± 1.2 nm ($n = 150$).

Moreover, a longitudinal section of microfibrils shows an asymmetric topography distribution of the beads. Thus, beads seem to be composed of two parts, the bead itself, which corresponds to the higher part of 10 nm, and which we have named the primary bead and a secondary bead located on one side of the primary one and with a height around 5 nm (4.8 ± 0.6 nm) (fig 2). In one microfibril all secondary beads are on the same side of the primary beads. We also observed this for certain rotary shadowing micrographs (fig 4A). Without the height information, we could still see the primary bead, secondary bead and interbead. These interbeads (rotary shadowing named) are composed of the secondary bead and interbead (AFM named).

In 1988, Wright and Mayne described six to eight arms connecting beads on partially disrupted micro-

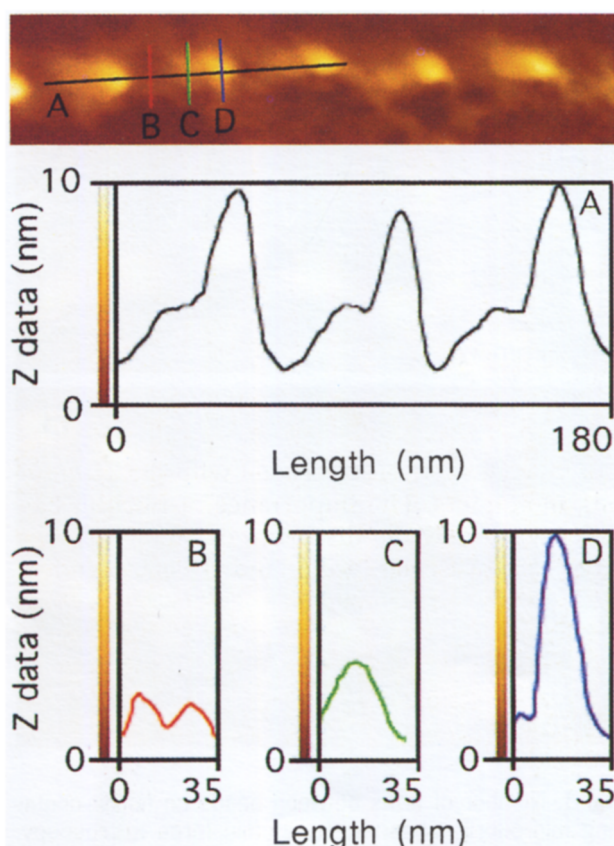


Fig 2. Sections of fibrillin-rich microfibrils. **A.** Longitudinal section on the microfibrillar axial level: microfibrils exhibit a three-level pattern, with the interbead with a height of approximately 2 nm; a second level named secondary bead with a height of approximately 5 nm and the primary bead represented by the higher level of 10 nm. **B.** Transversal section at the level of the interbead region: two different tops could be seen which represent the two arms described in figure 3. **C.** Transversal section at the level of the secondary bead: a single top with a height of approximately 5 nm is observed. **D.** Transversal section at the level of primary bead: the higher part of the microfibrils exhibit a height of 10 nm.

fibrils. AFM observations show arms between beads on native microfibrils. In this case the number of arms seems to be two or three (fig 3), with an height of about 2 nm (2.1 ± 0.3). In TEM observations, arms could only be seen with the same number (two or three) on stretched microfibrils (fig 4B). Furthermore, a unique arm was seen on very stretched microfibrils with a periodicity of around 200 nm (fig 4A).

DISCUSSION

Numerous works have investigated the thin structure of fibrillin-rich microfibrils. Biochemical techniques have been used to characterize the different components of these microfibrils and electron microscopy studies have partially allowed elucidation

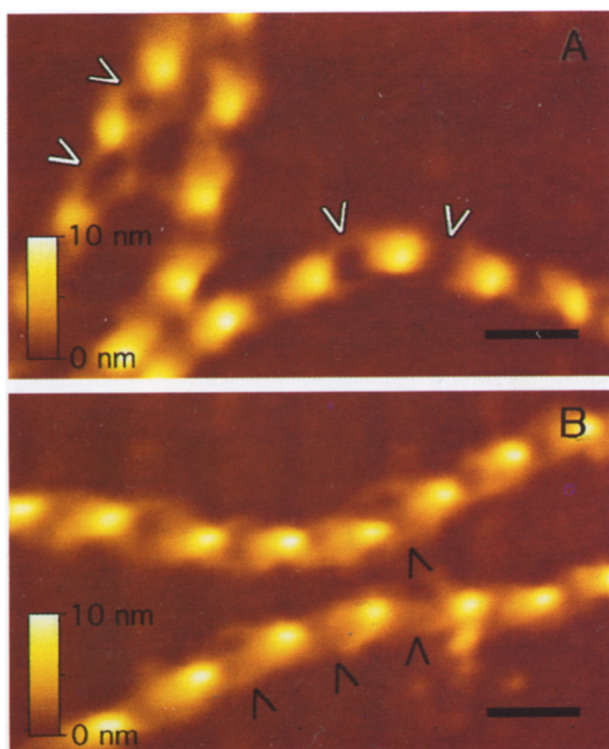


Fig 3. Number of arms between beads on fibrillin-containing microfibrils observed by atomic force microscopy. **A.** White arrows show two arms between beads. **B.** Black arrows show three arms between beads. Scale representing the sample height ranging from 0 to 10 nm. Scale bars, 50 nm.

tion of the organization of these components in microfibrils (Wright and Mayne, 1988; Keene *et al.*, 1991; Sakai *et al.*, 1991; Wallace *et al.*, 1991). It is now known that fibrillin, which is the major component of these microfibrils, is responsible for one of the major connective tissue diseases: Marfan syndrome (Dietz *et al.*, 1991; Lee *et al.*, 1991; Maslen *et al.*, 1991). This syndrome is characterized by a number of pathologies (Pyreritz, 1993), from ectopia lentis to skeletal deformation *via* cardiovascular fragility and aortic root dilatation. The comprehension of the microfibril ultrastructure could help to understand the mechanism of microfibril deficiency in the Marfan syndrome.

Fibrillin-rich microfibrils were easily identified. On the two-dimensional AFM image, their morphological pattern is the same as observed in transmission electron microscopy after rotary shadowing. Previous data showed that microfibrils in solution buffer with different ionic environment offered modification of their structure (Thurmond and Trotter, 1996), but our observations confirm that the microfibrils coated onto the mica prior to be washed with water would be less susceptible to ionic environment during this washing. Fibrillin-

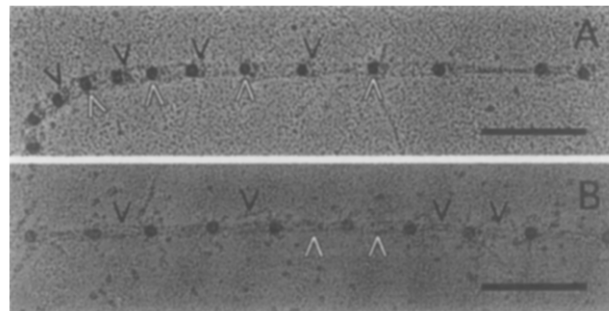


Fig 4. Transmission electron microscopic observation of fibrillin-rich microfibrils after rotary shadowing. **A.** Stretched microfibril exhibiting a periodicity ranging from 50 up to 200 nm. White arrows show the primary beads. Black arrows show the secondary beads which are slightly more electron-dense than interbead region. **B.** Stretched microfibrils with a 100 nm periodicity. The number of arms can be seen between beads. This number seems to be from 2 to 3. White arrows show interbeads with two arms, black arrows show interbeads with three arms. Scale bars, 200 nm.

containing microfibrils exhibit a periodic beaded-structure with a periodicity of 50 to 60 nm. With transmission electron microscopy, native microfibrils showed a beaded-structure with a periodicity of about 50–55 nm, which increases to about 80 nm on stretched microfibrils (Keene *et al.*, 1991). This periodicity was enhanced by immunolabeling with monoclonal antibody (mAb) raised against fibrillin-1 (Sakai *et al.*, 1991). Complementary immunostainings of microfibrils with mAb raised against recombinant fib-1 peptides led us to propose a model of a non-staggered head-to-tail alignment of fibrillin monomers inside the microfibrils (Reinhardt *et al.*, 1996). These immunostainings are also in agreement with a staggered model (Downing *et al.*, 1996). However, Handford *et al.* (1995) have suggested an anti-parallel alignment of monomers based on the study of the crystal-packing of two EGF-like domains. However, this model was not in agreement with the previous results (Reinhardt *et al.*, 1996). Because of the 148 nm long flexible rod-like structure of the fibrillin monomer, it had been proposed that beads contain the overlapping C and N-terminal regions of fibrillin and represent the sites at which other components, such as MAGP-1, are associated to fibrillin monomers (Sakai *et al.*, 1991; Henderson *et al.*, 1996). As the 148-nm length of fibrillin monomer was more than twice the microfibril periodicity, about half of each monomer must be overlapped with half of the following monomer. However, in rotary shadowing, we have observed some microfibrils with a periodicity of more than 150 nm up to 200 nm (fig 4). This result contradicts the suggested overlapping model.

One of the main interests of AFM is its ability to investigate biological material in its native state, for example collagen (Revenko *et al*, 1994) or actine (Henderson *et al*, 1992), avoiding all processing such as fixation, dehydration, embedding, sectioning and staining. However, the resolution depends on both the relief of the sample and the geometry of the tip (Stemmer and Engel, 1990; Blackford *et al*, 1991). The consecutive artefact, named convolution, affects the width of the sample but not the height. As a consequence of tip artefacts, the width of microfibrils determined by AFM was clearly larger (30 to 35 nm) than after rotary shadowing (25 nm). But the apparent height of microfibrils at the level of the beads (9.5 ± 1.2 nm) is in agreement with the microfibrillar diameter observed in ultrathin sections (apparent height, because it could arise from artefactual interactions between the tip and the sample). But in non-contact mode, these interactions are much less important than in tapping mode (Van Noort *et al*, 1997) because in theory, the tip is never in contact with the sample. Then, the diameter of microfibrils would be 10 nm and the elevated values obtained after rotary shadowing (25 nm) could be due to the shadowing metal overloading. Nevertheless, our conclusions concerning the real microfibrils' diameter do not take into account the AFM measured diameter which could include artefacts due to the tip sharpness.

Longitudinal and transversal sections show that interbeads are made of two parts. However, all the beads of a microfibril have their tops oriented in the same direction. This asymmetric pattern of microfibrils has been described previously by Sherratt *et al* in 1997 on STEM analysis, as an asymmetric mass distribution. Our results are in agreement with this work with an asymmetric topography distribution. On a given image, this orientation varies from one microfibril to another, excluding the possibility of a technical artefact, but strengthening the model of microfibril where monomers are arranged in a 'head-to-tail' parallel manner. The asymmetrical structure of beads could be a consequence of at least two structural hypotheses. Firstly, the folding of the fibrillin monomers could generate a higher topography on one side of the beads. Secondly, some associated components, such as MAGP-1, could be located in the higher part of each bead. This assumption is in agreement with the immunolabeling (Henderson *et al*, 1996) which located MAGP-1 at the level of the beads.

AFM experiments allowed us to visualize two or three arms between the beads of microfibrils. These data are not exactly in agreement with previous observations (Wright and Mayne, 1988) according to which, after rotary shadowing, six to eight arms emerged from each bead. However, these observations were performed on partly disrupted microfibrils. Indeed, the arms detected by AFM on unstret-

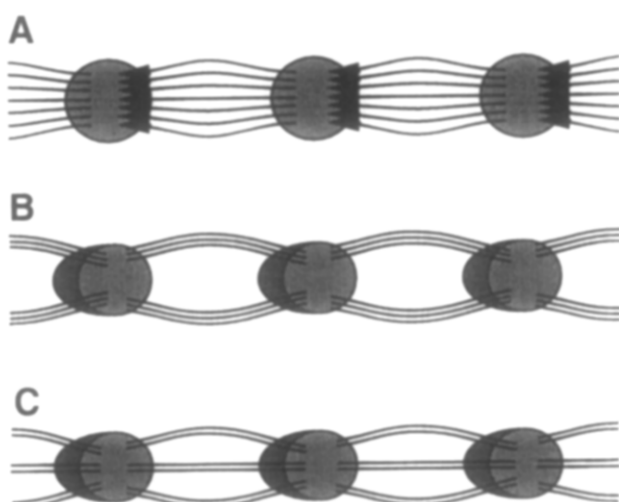


Fig 5. Modeling of monomer association inside microfibrils. **A.** Model proposed by Sakai *et al* (1991). **B.** Modeling of microfibrils on the basis of the untaggered model, with monomers associated in trimers. **C.** Modeling of microfibrils on the basis of the untaggered model, with monomers associated as dimers. Up to now it is impossible to state if the N-terminus and the C-terminus are located in the primary bead (clear gray) or in the secondary bead (dark gray).

ched microfibrils and by rotary shadowing on stretched microfibrils will not correspond to the number of monomers forming the microfibrillar interbeads but rather to the association of monomers between them as suggested by the two complementary models (fig 5). This hypothesis is supported by the fact that aggregation of two monomers is the first step in microfibril formation (Kiely and Shuttleworth, 1993). However, the height of the arms, around 2 nm, that we have found, corresponds to the 2.2 nm in width of fibrillin monomer as observed after rotary shadowing (Sakai *et al*, 1991).

Our observations demonstrate that microfibril beads are made of two different parts, in contrast to previous results in which beads are observed as simple structure. These two different parts are probably heterogeneous in composition and involved in the elastic function. We also demonstrate that the interbead region is composed of two or three arms, probably composed by fibrillin dimers or trimers which have never been previously described. These two results led us to propose a complementary model of monomer aggregation within microfibrils based on a model previously described (Sakai *et al*, 1991). Further AFM observations using antibodies raised against different parts of monomer, as C-terminus or N-terminus, or against microfibril-associated component as MAGP-1, could give us their exact locations within microfibrils.

ACKNOWLEDGMENTS

This work has been supported by the European grant BIO4-CT96-0662. E Hanssen is supported by funds from the 'Ministère de l'Education Nationale et de l'Enseignement Supérieur'. We would like to thank Doctor Antony Coleman for his technical assistance and discussion in AFM experiments and Doctor Josef Deutscher for helpful discussion.

REFERENCES

- Baselt DR, Revel JP and Baldeschweiler JD (1993) Subfibrillar structure of type I collagen observed by atomic force microscopy. *Biophys J* 65, 2644–2655
- Binnig G, Quate CF and Gerber CH (1986) Atomic force microscope. *Phys Rev Lett* 56, 930–933
- Blackford BL, Jericho MH and Mulhern PJ (1991) A review of scanning tunneling microscope and atomic force microscope imaging of large biological structures: problems and prospects. *Scanning Microscopy* 5, 907–918
- Bressan GM, Daga-Gordini D, Colombatti A, Castellani I, Marigo V and Volpin D (1993) Emilin, a component of elastic fibers preferentially located at the elastin-microfibrils interface. *J Cell Biol* 121, 201–212
- Chernoff EAG and Chernoff DA (1992) Atomic force microscope image of collagen fibers. *J Vac Sci Technol* 10, 596–599
- Dietz HC, Cutting GR, Pyeritz RE, Maslen CL, Sakai LY, Corson GM, Puffenberger EG, Hamosh A, Nanthakumar EJ, Currin SM, Stetten G, Meyers DA and Francomano CA (1991) Marfan syndrome caused by a recurrent *de novo* missense mutation in the fibrillin gene. *Nature* 352, 337–339
- Downing AK, Knott V, Werner JM, Cardy CM, Campbell ID and Handford PA (1996) Solution structure of a pair of calcium-binding epidermal growth factor-like domains: implications for the Marfan syndrome and other genetic disorders. *Cell* 85, 597–605
- Gibson MA and Cleary EG (1987) The immunohistochemical localization of microfibril-associated glycoprotein (MAGP) in elastic and non-elastic tissues. *Immunol Cell Biol* 65, 345–356
- Gibson MA, Hatzinikolas G, Davis EC, Baker E, Sutherland GR and Mecham RP (1995) Bovine latent transforming growth factor β 1-binding protein-2: molecular cloning, identification of tissue isoforms, and immunolocalization to elastin-associated microfibrils. *Mol Cell Biol* 15, 6932–6942
- Gibson MA, Hatzinikolas G, Kumaratilake JS, Sandberg LB, Nicholl JK, Sutherland GR and Cleary EG (1996) Further characterization of protein associated with elastic fiber microfibrils including the molecular cloning of MAGP-2 (MP25). *J Biol Chem* 271, 1096–1103
- Handford P, Downing AK, Rao Z, Hewett DR, Sykes BC and Kielty CM (1995) The calcium binding properties and molecular organization of epidermal growth factor-like domains in human fibrillin-1. *J Biol Chem* 270, 6751–6756
- Henderson E, Haydon PG and Sakaguchi DS (1992) Actin filament dynamics in living glial cells imaged by atomic force microscopy. *Science* 257, 1944–1946
- Henderson M, Polewski R, Fanning JC and Gibson MA (1996) Microfibril-associated glycoprotein-1 (MAGP-1) is specifically located on the beads of the beaded-filament structure for fibrillin-containing microfibrils as visualized by the rotary shadowing technique. *J Histochem Cytochem* 44, 1389–1397
- Kagan HM, Vaccaro CA, Bronson RE, Tang SS and Brody JS (1986) Ultrastructural immunolocalization of lysyl-oxidase in vascular connective tissue. *J Cell Biol* 103, 1121–1128
- Keene DR, Sakai LY and Burgeson RE (1991) Human bone contains type III collagen, Type VI collagen, and fibrillin: type III collagen fibers that may mediate attachment of tendons, ligaments, and periosteum to calcified bone cortex. *J Histochem Cytochem* 39, 59–69
- Kielty CM and Shuttleworth CA (1993) Synthesis and assembly of fibrillin by dermal fibroblasts and smooth muscle cells. *J Cell Sci* 106, 167–173
- Kielty CM, Whittaker SP and Shuttleworth CA (1996) Fibrillin: evidence that chondroitin sulfate proteoglycans are components of microfibrils and associated with newly synthesised monomers. *FEBS Lett* 386, 169–173
- Kielty CM, Hanssen E and Shuttleworth CA (1998) Purification of fibrillin-containing microfibrils and collagen VI microfibrils by density gradient centrifugation. *Anal Biochem* 255, 108–112
- Kikuchi Y, Tsuchikura O, Hirama M and Tamiya N (1987) Desmosine and isodesmosine as cross-links in the hinge-ligament protein of bivalves. 3,3'-Methylenebistysine as an artefact. *Eur J Biochem* 164, 397–402
- Lee B, Godfrey M, Vitale E, Hori H, Mattei M-G, Sarfarzi M, Tsipouras P, Ramirez F and Hollister DW (1991) Linkage of Marfan syndrome and a phenotypically related disorder to two different fibrillin genes. *Nature* 352, 330–334
- Maslen LC, Corson GM, Maddox BK, Glanville RW and Sakai LY (1991) Partial sequence of a candidate gene for the Marfan syndrome. *Nature* 352, 334–337
- Mould AP, Holmes DF, Kadler KE and Chapman JA (1985) Mica sandwich technique for preparing macromolecules for rotary shadowing. *J Ultrastruct Res* 91, 487–492
- Pyeritz RE (1993) The Marfan syndrome. In: *Connective tissue and its heritable disorders, molecular, genetic, and medical aspects* (Royce MP and Steinmann B, eds) Wiley-Liss, New-York, 437–468
- Reinhardt DP, Keene DR, Corson GM, Pöschl E, Bächinger HP, Gambee JE and Sakai LY (1996) Fibrillin-1: Organization in microfibrils and structural properties. *J Mol Biol* 258, 104–116
- Revenko I, Sommer F, Tran Minh D, Garrone R and Franc J-M (1994) Atomic force microscopy of the collagen fibre structure. *Biol Cell* 80, 67–69
- Roark EF, Keene DR, Haudenschild CC, Godyn S, Little CD and Argraves WS (1995) The association of human fibulin-1 with elastic fibers: an immunohistological, ultrastructural, and RNA study. *J Histochem Cytochem* 43, 401–411
- Robert L and Robert AM (1980) Biology and pathology of elastic tissues. *Front Matrix Biol* 8, 130–173
- Rosenbloom J, Abrams WR and Mecham R (1993) Extracellular matrix 4: the elastic fiber. *FASEB J* 7, 1208–1218
- Sakai LY, Keene DR and Engvall E (1986) Fibrillin, a new 350-kDa glycoprotein, is a component of extracellular microfibrils. *J Cell Biol* 103, 2499–2509
- Sakai LY, Keene DR, Glanville RW and Bächinger HP (1991) Purification and partial characterization of fibrillin, a cysteine-rich structural component of connective tissue microfibrils. *J Biol Chem* 266, 14763–14770
- Sheratt MJ, Holmes DF, Shuttleworth CA and Kielty CM (1997) Scanning transmission electron microscopy mass analysis of fibrillin-containing microfibrils from foetal elastic tissues. *Int J Biochem Cell Biol* 29, 1063–1070
- Stemmer A and Engel A (1990) Imaging biological macromolecules by STM: quantitative interpretation of topographs. *Ultramicroscopy* 34, 129–140
- Thurmond FA and Trotter JA (1996) Morphology and biomechanics of the microfibrillar network of sea cucumber dermis. *J Exp Biol* 199, 1817–1828
- Van Noort SJT, Van der Werf KO, De Groot BG, Van Hulst NF and Greve J (1997) Height anomalies in tapping mode atomic force microscopy in air caused by adhesion. *Ultramicroscopy* 69, 117–127
- Vitellaro-Zuccarello L, De Biasi S and Bairati A (1983) The ultrastructure of the byssal apparatus of a mussel. V. Localization of collagenic and elastic components in the threads. *Tissue Cell* 15, 547–554
- Wallace RN, Streeten BW and Hanna RB (1991) Rotary shadowing of elastic system microfibrils in the ocular zonule, vitreous, and ligamentum nuchae. *Curr Eye Res* 10, 99–109
- Wright DW and Mayne R (1988) Vitreous humour of chicken contains two fibrillar systems: an analysis of their structure. *J Ultrastruct Mol Struct Res* 100, 224–234
- Xu M and Lewis RV (1990) Structure of a protein superfiber: spider dragline silk. *Proc Natl Acad Sci USA* 87, 7120–7124

Received 12 January 1998; accepted 18 May 1998